UNIVERSITY OF MISKOLC
FACULTY OF MECHANICAL ENGINEERING AND INFORMATICS

NUMERICAL SIMULATION OF THE HEAT AND MASS FLOW OF A SOLAR COLLECTOR APPLYING ALTERNATIVE LIQUIDS

PHD THESES

Prepared by

Mustafa Moayad Hasan
Mechanical Engineering Department (BSc),
Mechanical Engineering Department (MSc)

ISTVÁN SÁLYI DOCTORAL SCHOOL OF MECHANICAL ENGINEERING SCIENCES
TOPIC FIELD OF BASIC ENGINEERING SCIENCES
TOPIC GROUP OF TRANSPORT PROCESSES AND MACHINES

Head of Doctoral School

Dr. Gabriella Bognár
DSc, Full Professor

Head of Topic Group

Dr. László Baranyi
Full Professor

Scientific Supervisor

Dr. Krisztián Hriczó
Associated professor

Miskolc
2025

JUDGING COMMITTEE

Chair:

Secretary:

Members:

OFFICIAL REVIEWERS

1. INTRODUCTION

1.1. Solar Energy Technologies

In the face of challenges posed by traditional fossil fuels, such as scarcity, price volatility, and environmental damage, renewable energy sources have become critical [1]. Among these, solar energy stands out as a clean, abundant, and carbon-free option. Technologies to harness solar energy are broadly divided into two categories:

- **Photovoltaic (PV) Systems:** These directly convert sunlight into electricity using the photovoltaic effect. While effective, the efficiency of PV panels decreases as their temperature rises due to the conversion of infrared radiation into thermal energy.
- **Solar Thermal (ST) Systems:** These systems capture the sun's radiant heat to warm a fluid (liquid or air). This thermal energy can be used for space heating, water heating, and cooling applications.

A common type of ST system is the Flat-Plate Solar Collector (FPSC), valued for its simple design, low maintenance, and cost-effectiveness. However, FPSCs face challenges, including significant heat loss and a low heat transfer coefficient between the collector's absorber plate and the circulating fluid, which limits their thermal efficiency.

1.2. The Dual-Purpose Solar Thermal Collector (DPSTC)

To overcome the limitations of conventional FPSCs, a novel design known as the Dual-Purpose Solar Thermal Collector (DPSTC) has been developed. A DPSTC is a single unit that combines two solar thermal technologies, typically an air heater and a liquid heater, into one device. It features two separate, sealed channels, one for heating air and one for heating a liquid, allowing it to generate hot air and hot liquid either simultaneously or separately [2].

The primary benefits of DPSTC include:

- Increased thermal performance and utilization of solar energy.
- Reduced installation area and lower overall costs.
- Effective heat delivery for achieving high temperatures.

DPSTCs can be categorized into two main types based on their installation:

- **Freestanding DPSTCs:** Installed independently in open spaces for residential, industrial, or agricultural use.
- **Building-Integrated DPSTCs:** Integrated into the building envelope (e.g., roofs or facades) to provide space heating, water heating, and reduce the building's energy consumption.

This research focuses on the numerical simulation and optimization of a freestanding DPSTC to enhance its thermal performance. Figure 1.1 shows the classification of dual-function collectors.

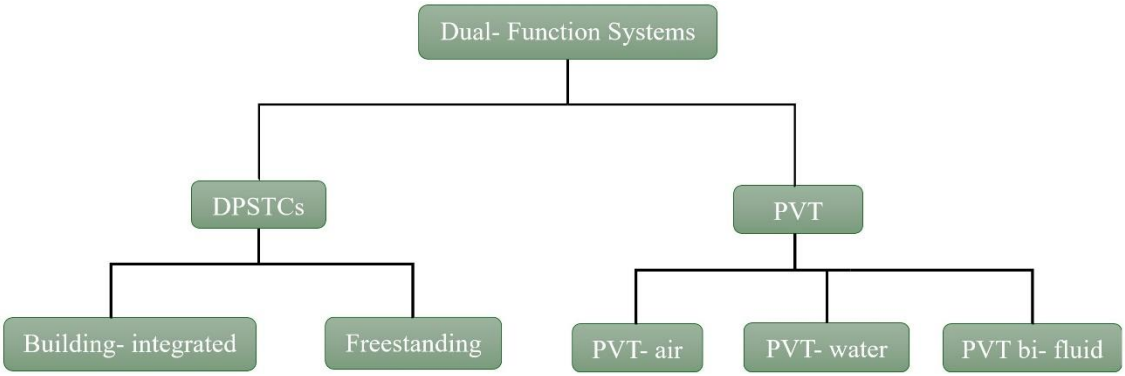

Figure 1.1. Classification of dual-function solar energy systems.

1.3. Enhancing Performance with Alternative Fluids

The efficiency of any solar thermal system is highly dependent on the Heat Transfer Fluid (HTF) that circulates through it to capture and transport solar energy. While water is the most common HTF, it has limitations, including poor thermal properties at extreme temperatures (freezing and boiling) and the potential for scale formation [3].

To improve performance, researchers have explored alternative fluids:

- **Oil-Based Fluids:** Industrial oils like Therminol and Dowtherm offer better thermo-physical properties than water and can operate at much higher temperatures, making them suitable for industrial applications [4].
- **Nanofluids:** These are engineered fluids containing nano-sized solid particles (e.g., metal oxides like CuO or carbon nanotubes like MWCNT) suspended in a base fluid like water. Nanofluids exhibit significantly enhanced thermal conductivity and heat transfer capabilities [5].
- **Hybrid Nanofluids (HNFs):** These fluids combine different types of nanoparticles in a single base fluid to leverage the synergistic effects of the materials, further improving thermophysical and optical properties [6].

A central goal of this thesis is to investigate how these alternative fluids can improve the performance of a DPSTC, a topic that has not been extensively explored in existing literature.

2. METHODOLOGY

2.1. Mathematical and Numerical Approaches

To analyze the complex thermal behavior of the DPSTC, this research employs a combination of mathematical modeling and advanced numerical simulation.

Mathematical Modeling: The performance of the DPSTC is primarily evaluated by its useful heat gain ($Q_{u,DPSC}$), which is the difference between the solar energy absorbed by the collector and the total heat lost to the environment as [7]:

$$Q_{u,DPSC} = Q_{u,\,water} + Q_{u,\,air}\,. \tag{2.1}$$

Key mathematical concepts used in this analysis include:

- **Heat Removal Factor (F_R):** A crucial parameter that relates the actual useful heat gain to the theoretical maximum gain if the entire collector were at the fluid's inlet temperature [8].

$$F_R = \frac{\varepsilon_f\, \dot{m}_f\, C_{p,f}}{U_L\, A_c + \varepsilon_f\, \dot{m}_f\, C_{p,f}}\,. \tag{2.2}$$

- **Effectiveness-NTU (ε-NTU) Method:** A standard heat exchanger analysis technique used to determine the performance of the collector. A novel aspect of this thesis is treating the DPSTC as a parallel flow heat exchanger, which simplifies the analysis and eliminates iterative calculations required by other methods [9].

$$\varepsilon_f = \frac{1-exp[(-h_f\, A_f/C_{min.})(1+C_{min.}/C_{max.})]}{(1+C_{min.}/C_{max.})}, \tag{2.3}$$

These mathematical models were implemented and solved using custom codes developed in MATLAB.

2.2. Simulation and Validation

For a more detailed investigation of fluid flow and heat transfer, Computational Fluid Dynamics (CFD) was employed using the ANSYS Fluent software package.

- **CFD Model:** A three-dimensional model of the DPSTC was created, consisting of a glass cover, an absorber plate, seven parallel liquid tubes, and seven V-corrugated air channels. To optimize computational resources, a symmetrical half-section of a single air duct and liquid tube was modeled (see Figure 2.1).

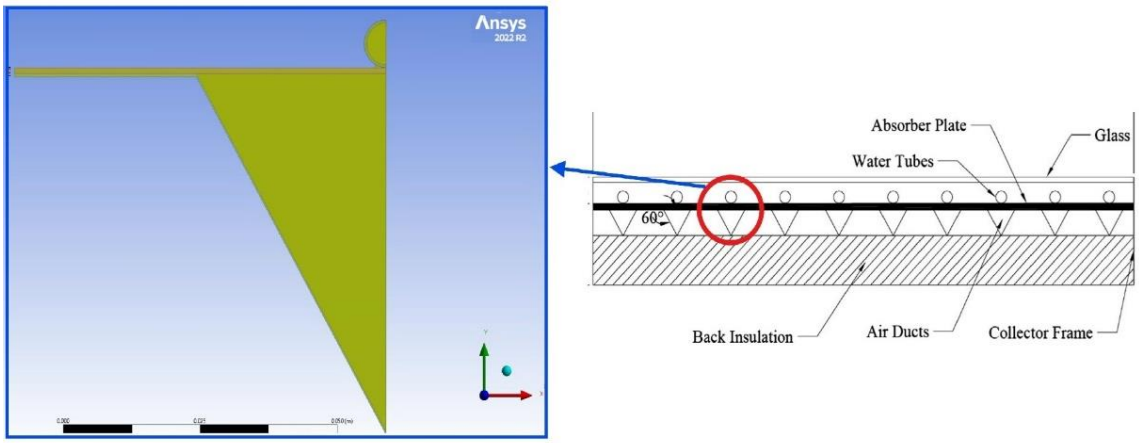

Figure 2.1. The cross-sectional view of the DPSC and its corresponding ANSYS model.

- **Mesh Generation and Independence:** A high-quality conformal mesh was generated, consisting of tetrahedron elements with a structured mesh (prism layers) and a growth rate of 1.01. The boundary conditions of the studied model are defined by creating named selections in the Fluent meshing. A grid-independence test was performed to ensure that the simulation results were independent of the mesh size, confirming the reliability of the numerical model (see Figure 2.2).

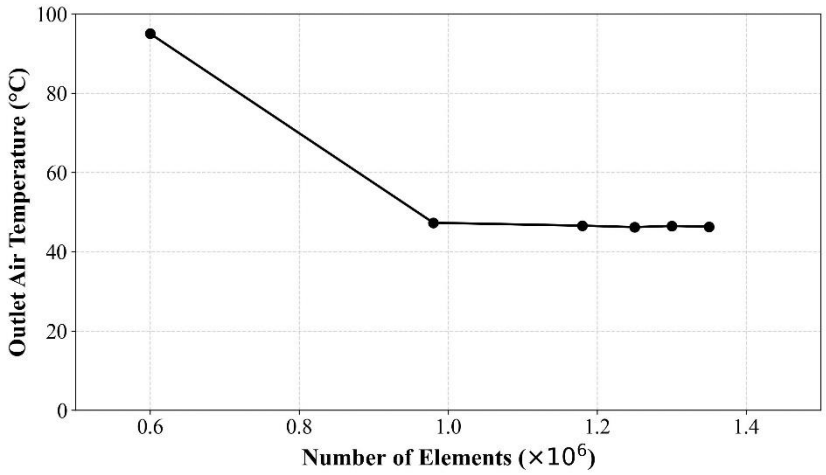

Figure 2.2. Mesh independence test.

- **Validation:** To ensure the accuracy of both the MATLAB and ANSYS models, the simulation results were rigorously validated against experimental data from published literature. The models were run using the same meteorological and operational conditions as the experiments. The close agreement between the simulated results and the experimental data, with minimal relative error, confirmed the validity and success of the developed models.

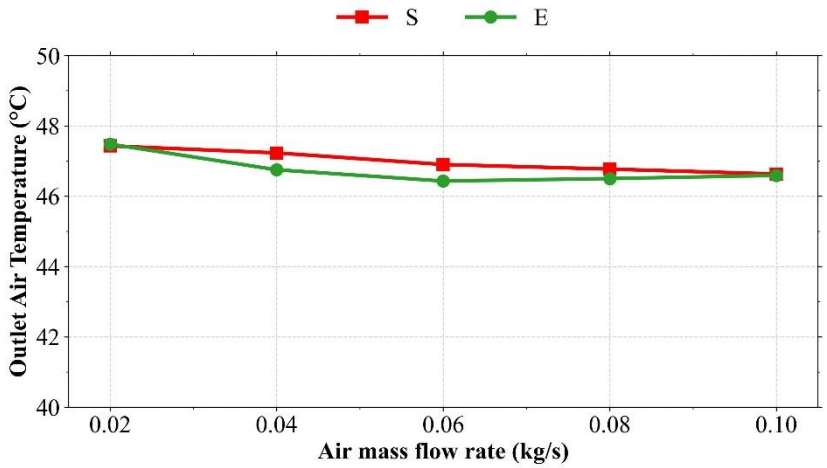

Figure 2.3. Validation of the present simulation results (S) against the experimental data (E) reported by Assari et al. [7].

2.3. Friction Factor, Pumping Power, Collector Area, and Energy–Emission Analysis

The friction factor (f) for all the examined liquids in the simulation is determined by the following equation [10]:

$$f = \frac{\Delta P}{\left(\frac{L}{D}\right)\left(\frac{\rho v^2}{2}\right)}, \tag{2.4}$$

here L, D, ρ, and v denote the pipe length, pipe diameter, liquid density, and liquid flow velocity, respectively. The pumping power (W_P) required to circulate the fluid, influenced by flow rate, pipe roughness, and fittings, is defined as [10]:

$$W_P = \Delta P \left(\frac{\dot{m}}{\rho}\right). \tag{2.5}$$

This study aims to evaluate whether using different HTFs instead of water in DPSTC can reduce collector size, leading to cost savings and more efficient use of installation space. The reduction in the collector area (A_{red}) is given as [11]:

$$A_{red} = \frac{\dot{m}_f \, C_{p,f} \left(T_{out,f} - T_{in,f}\right)}{\eta \, I_t \, (\tau\alpha)}. \tag{2.6}$$

3. DPSTC AS A PARALLEL FLOW HEAT EXCHANGER

3.1. A Novel Mathematical Framework

This chapter introduces a novel analytical approach for modeling the DPSTC, an area not previously explored in scientific literature. The core innovation is treating the DPSTC, with its dual channels for air and water, as a parallel flow heat exchanger [12].

This methodology is justified by the physical structure of the collector, where two separate fluids flow alongside each other, exchanging heat with the common absorber plate. By applying the standard effectiveness (ε) equation for parallel flow heat exchangers, a unique and simplified mathematical framework was developed. A comprehensive MATLAB code was created to simulate the DPSTC based on this new model. The simulation process involves:

- Inputting design parameters and meteorological data.
- Making an initial estimation of the absorber plate temperature.
- Calculating heat loss coefficients, Reynolds (Re) and Nusselt (Nu) numbers, and heat transfer coefficients (h) for both air and water.
- Determining the effectiveness (ε_f), number of transfer units (NTU), and heat removal factor (F_R).
- Calculating the useful heat gain (Q_u) and the outlet temperatures for both fluids.
- Iterating the process by recalculating the plate temperature until convergence is achieved.

3.2. Accuracy and Predictions

The reliability of this new mathematical framework was tested by comparing its simulation results with experimental data from a study by Nematollahi et al. [13]. The accuracy was quantified using Relative Percentage Error (RPE) and Average Relative Percentage Error (ARPE) for key parameters like absorber plate temperature, water outlet temperature, and useful heat gain (see Table 3.1).

Table 3.1. Comparison of Experimental Data [13] and Predicted Data (This Work) for Absorber Temperature, Water Outlet Temperature, and Useful Heat Gain with Corresponding RPE and ARPE.

Absorber Temperature, (°C)			Water outlet Temperature, (°C)			Useful heat absorbed, (W)		
Experimental Data [13]	Predicted Data (This Work)	Relative Error (%)	Experimental Data[13]	Predicted Data (This Work)	Relative Error (%)	Experimental Data [13]	Predicted Data (This Work)	Relative Error (%)
50.97	60.49	2.94	46.97	52.82	12.46	1253.90	1382.44	10.25
57.35	63.44	1.84	53.94	55.52	2.93	1615.60	1588.79	1.66
62.94	67.74	1.43	60.04	57.79	3.74	1730.50	1676.27	3.13
66.50	69.17	0.79	64.03	59.17	7.58	1632.62	1659.67	1.66
68.53	70.05	0.44	67.01	65.09	2.86	1441.13	1579.07	9.57
70.78	71.96	0.34	70.05	70.32	0.38	1113.48	1352.95	21.51
71.94	77.55	1.63	71.94	70.52	1.97	791.49	895.06	13.09
ARPE		1.3			4.5			8.6

Key Findings:

- The absorber plate and water outlet temperatures increase steadily with rising solar intensity, showing similar trends. Simulated absorber temperatures were slightly higher than experimental values due to simplified heat-loss assumptions and absorber design effects. The maximum RPE reached 2.94% (plate) and 12.46% (water), while ARPE values were 1.3% and 4.5%, indicating greater deviation in outlet water temperatures.
- The predicted useful energy showed good agreement with experimental results, with maximum RPE and ARPE values of 21.51% and 8.6%, respectively. Deviations arise mainly from estimated effectiveness, optical properties, and heat-loss assumptions affecting heat gain accuracy. Overall, the model demonstrates reliable convergence with experimental data.
- The discrepancies observed were attributed to the use of averaged meteorological data in the simulation and estimations made for material properties (like thermal conductivity of insulation) that were not specified in the experimental study.

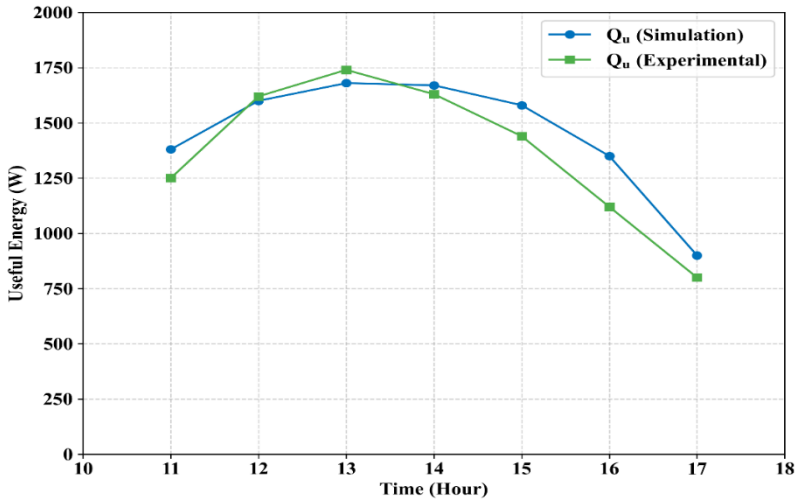

Figure 3.1. Variation of useful heat gain over time: comparison of Simulation (This work) and Experimental data [13].

As a summary, treating the DPSTC as a parallel flow heat exchanger and analyzing it with the ε-NTU method proved to be a reliable and stable model for predicting collector performance. This novel approach simplifies the analytical process and provides accurate results, underscoring its value for future research.

4. OPTIMAL ANALYSIS METHODOLOGIES

4.1. Developing and Comparing Three Models

To identify the most accurate and efficient method for analyzing a DPSTC, this chapter develops and compares three distinct mathematical approaches, each implemented in a separate MATLAB code (C1, C2, and C3). The goal was to refine the calculation of the heat removal factor (F_R), which is essential for determining the collector's effective heat gain [14].

The three models were:

- Code C1 (Standard ε-NTU Method): This approach used a common effectiveness equation from the literature to calculate the heat removal factor (F_R). This is a widely used method by researchers.
- Code C2 (Single-Purpose Method): This model calculated the heat removal factor using an equation specific to a DPSTC operating in a single mode (e.g., only water heating or only air heating).
- Code C3 (Novel Parallel Flow Method): This was the innovative approach from, which treated the DPSTC as a parallel flow heat exchanger. Instead of using the heat removal factor, it directly implemented the effectiveness equation for parallel flow to calculate the useful heat gain.

To the best of our knowledge, this was the first time these three distinct analyses were conducted and compared simultaneously for a DPSTC.

4.2. Performance and Model Selection

All three codes were validated against experimental data from a study by Saleh and Jasim [15]. To quantitatively assess their accuracy, two error metrics were calculated: Root Mean Square Error (RMSE) and Mean Absolute Error (MAE), expressed mathematically as [16]:

$$MAE = \frac{1}{n}\sum_{i=1}^{n} |(T_{out,(S)} - T_{out,(E)})|. \quad (4.1)$$

$$RMSE = \sqrt{\frac{1}{n}\sum_{i=1}^{n}(T_{out,(S)} - T_{out,(E)})^2}. \quad (4.2)$$

- **Air Outlet Temperature:** Code C3 demonstrated significantly better predictions. The RMSE values for C1, C2, and C3 were 3.4%, 3.8%, and **1.8%**, respectively. The MAE values were 3.0%, 3.3%, and **1.5%**.
- **Water Outlet Temperature:** Code C3 again proved superior. The RMSE values were 0.8%, 1.7%, and **0.3%**, and the MAE values were 0.7%, 1.4%, and **0.3%** for C1, C2, and C3, respectively.

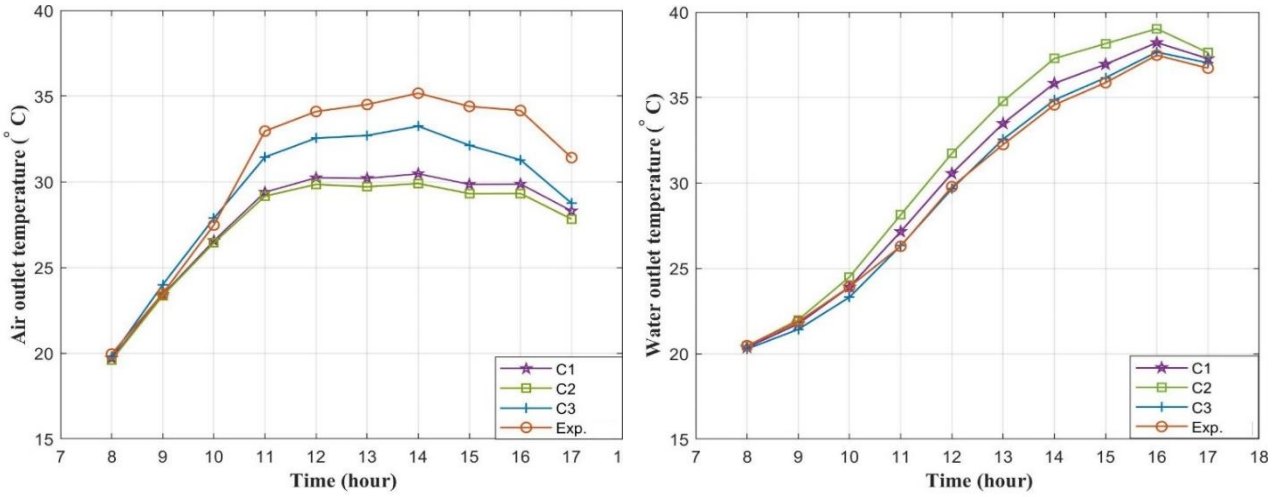

(a) (b)

Figure 4.1. Variation of (a) air and (b) water outlet temperatures over time for the three codes.

The results clearly showed that Code C3 outperformed the other two models, exhibiting the lowest error values for both water and air outlet temperatures. This confirms that treating the DPSTC as a parallel flow heat exchanger is the most accurate and reliable analytical approach. This finding is a significant contribution, providing future researchers with an optimized and validated mathematical tool for studying DPSTCs.

5. NUMERICAL INVESTIGATION OF OIL-BASED LIQUIDS

5.1. Simulation with Water, Therminol VP-1, and Dowtherm A

This chapter presents the first key innovation of the thesis: a Computational Fluid Dynamics (CFD) investigation into the use of alternative heat transfer fluids (HTFs) in a DPSTC, an area with a significant gap in the existing literature. The study, conducted using ANSYS Fluent, compared the performance of conventional water with two oil-based fluids: Therminol VP-1 and Dowtherm A [17]. These oils are particularly relevant for climates with extreme temperatures, as water is ineffective when it freezes (0°C) or boils (100°C).

Throughout the simulation, I analyzed how various airflow rates impacted exit temperatures, heat gains, and the thermal efficiency of the DPSTC. The input boundary conditions employed in the simulation are detailed in Table 5.1.

Table 5.1. Input parameters and their corresponding values used in the numerical simulation, as reported in Ref. [7].

Input parameter	Range
Solar irradiance	900 W/m^2
Inlet air temperature	45 °C
Inlet liquid temperature	40 °C
Air flow rate	0.02-0.1 kg/s
Liquid flow rate	0.02 kg/s

A total of 15 simulations were conducted to analyze the impact of airflow on the collector's performance with each of the three liquids.

5.2. Effects on Temperature, Heat Gain, and Efficiency

The simulation results revealed the significant advantages of using oil-based fluids over water in a DPSTC:

- **Exit Liquid Temperature:** Therminol and Dowtherm achieved much higher outlet temperatures than water. For example, at an airflow of 0.02 kg/s , the exit temperatures were approximately 52.5°C for Therminol and 52°C for Dowtherm, compared to only 45.6°C for water.

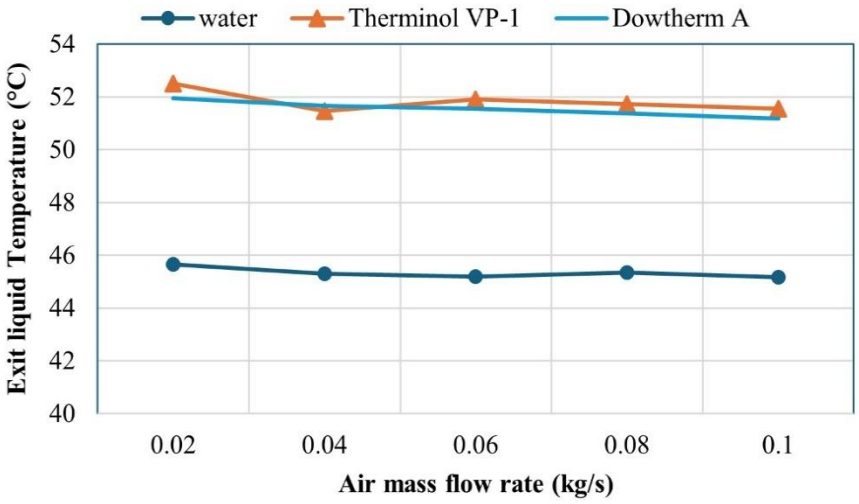

Figure 5.1. The variation of exit liquid temperature with air flow rates.

- **Heat Gain:** While water absorbed more heat on the liquid side due to its higher heat capacity, the total heat gain (liquid + air) was significantly higher for Therminol and Dowtherm. This is because the oils, having lower heat capacities, allowed the absorber plate to reach higher temperatures, which in turn transferred more heat to the air.

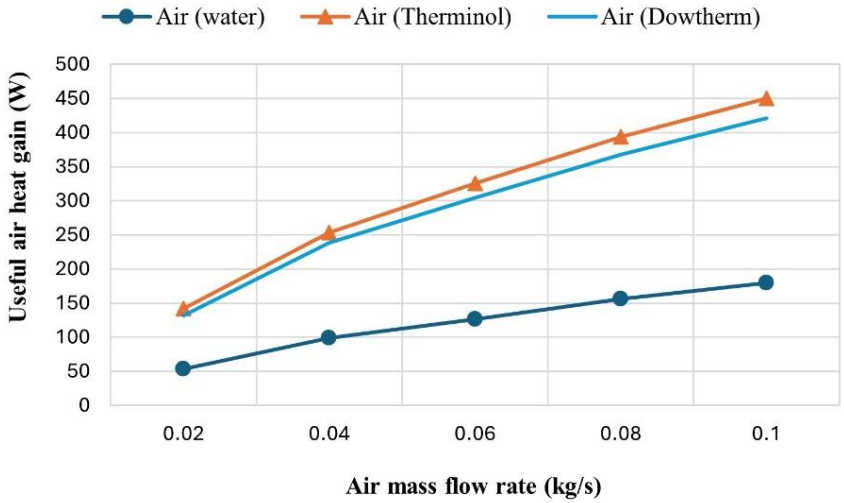

Figure 5.2. The variance of useful air heat gain with air flow rates.

- **Overall Efficiency:** Consequently, the total thermal efficiency of the DPSTC was greatest when using Therminol and Dowtherm. The efficiency increased with higher airflow rates for all fluids. At the maximum airflow of 0.1 kg/s , the total efficiencies reached approximately 52% for Therminol VP-1, 50% for Dowtherm A, and 38% for water.

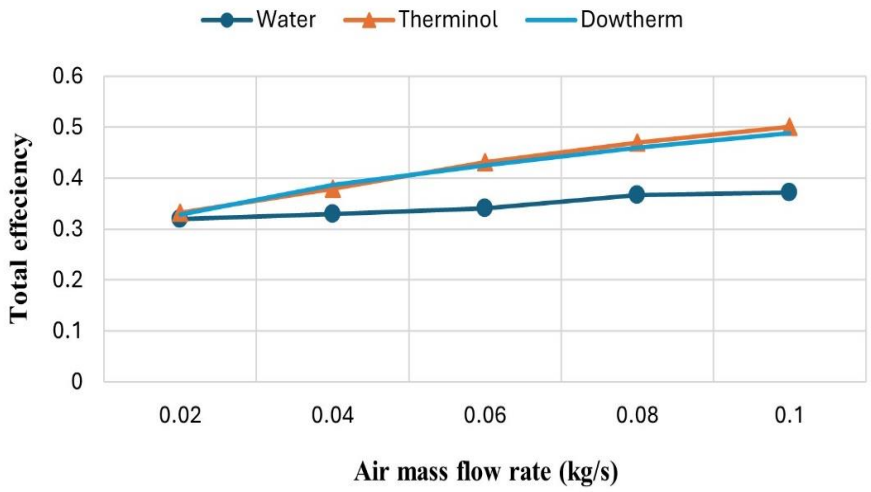

Figure 5.3. Total efficiency of the DPSTC with an air flow rate.

The total efficiency of the DPSTC is directly influenced by the increased airflow rate, particularly for both Therminol and Dowtherm liquids. Both liquids show a consistent increase in efficiency as the airflow rate rises, with the maximum efficiency recorded at 0.1 kg/s. This highlights the significant role of the airflow rate in the system's performance, as it influences the efficiency of both liquids.

In summary, using Therminol and Dowtherm instead of water significantly improves the overall thermal effectiveness of the DPSTC. While water provides better temperature uniformity, Therminol and Dowtherm yield higher absorber and outlet temperatures. Further studies should vary operating parameters, flow rates, and inlet temperatures to confirm the suitability of these alternative fluids. The next chapter explores nanofluids as potential replacements for oil-based liquids under similar conditions.

6. EVALUATION USING MONO-NANOFLUIDS

6.1. CFD Simulation with CuO-H_2O and MWCNT-H_2O

Building on the investigation of alternative fluids, this chapter explores the performance of a DPSTC using mono-nanofluids. This research is novel, as no prior studies have specifically examined the application of these nanofluids in DPSTCs. I employed nano fluids, specifically CuO-H_2O and MWCNT-H_2O, based on an extensive literature review identifying them as highly effective in solar collectors. Both were simulated at a 0.5% volume concentration using ANSYS Fluent. To facilitate the simulation, a MATLAB program was first developed to calculate the specific thermophysical properties of the nanofluids [18].

The investigation was conducted in two simulation phases:

1. **Varying Airflow:** The air flow rate was varied from 0.02 to 0.1 kg/s , while the liquid flow rate was held constant at 0.02 kg/s .
2. **Varying Liquid Flow:** The liquid flow rate was varied from 0.02 to 0.1 kg/s , while the air flow rate was held constant at 0.1 kg/s (identified as the optimal rate in phase 1).

To determine the thermophysical properties of the nanofluids, I developed a MATLAB program that enables the user to input a range of parameters, including all the properties outlined in Table 6.1, and the volume concentration of the selected nanoparticles. These inputs are then seamlessly substituted into the appropriate equations to compute the properties of the nanofluid. The calculated properties are carefully stored in a dedicated MATLAB workspace, ensuring they are readily available to serve as inputs for the ANSYS simulation during the definition of materials in the cell zone conditions [18].

Table 6.1. The thermo-physical properties of the base fluid and nanoparticles.

Physical properties	Water [19]	MWCNT [20]	CuO [21]
$\boldsymbol{\rho}$ (kg/m^3)	998.2	2100	6000
$\boldsymbol{k}$ (W/(m. K))	0.613	3000	33
$\boldsymbol{C_p}$ (J/(kg. K))	4182	519	551
$\boldsymbol{\mu}$ (mPa·s)	0.001	-	-

6.2. Impact of Flow Rates on Performance

The simulations demonstrated the remarkable thermal enhancement provided by the nanofluids compared to conventional water.

- **Outlet Temperatures:** Both nanofluids achieved significantly higher outlet liquid temperatures. At a liquid flow rate of 0.02 kg/s , they produced an outlet temperature of ~50°C, a 25% enhancement over the 40°C inlet, whereas water only achieved a 13%

increase. CuO-H_2O consistently showed slightly better performance than MWCNT-H_2O due to its higher heat capacity.

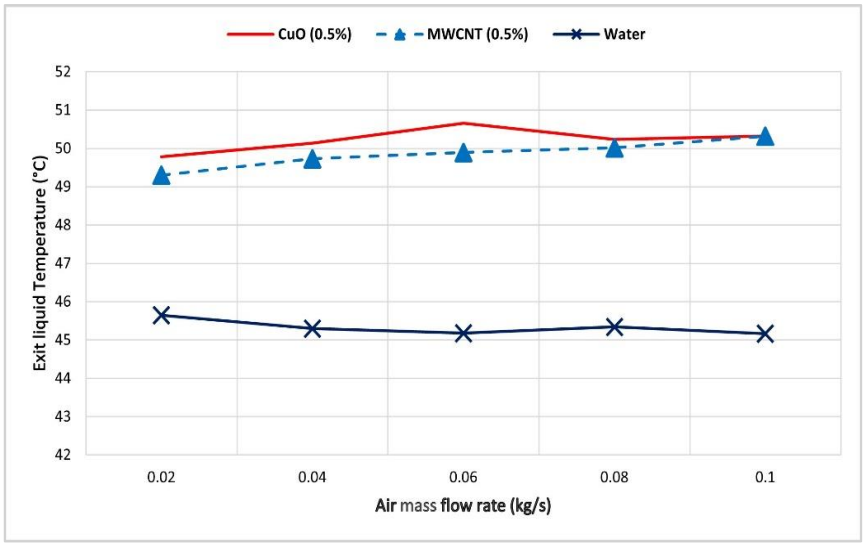

Figure 6.1. The effect of airflow rate on the exit liquid temperature for various HTLs.

- **Heat Gain:** The total useful heat gain increased with both air and liquid flow rates. The nanofluids substantially outperformed water. For instance, at the optimal flow rates (0.1 kg/s for both air and liquid), the maximum heat gain for CuO-H_2O was over 1650 W, compared to just over 1150 W for water.

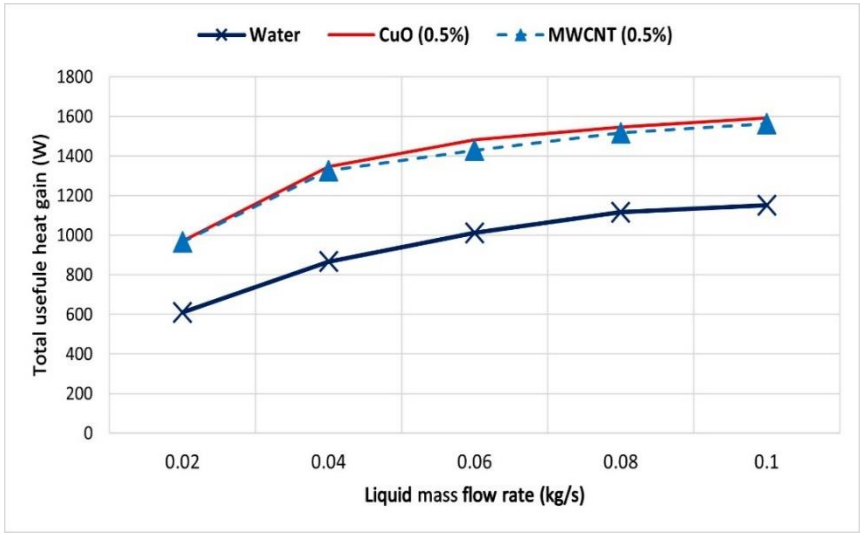

Figure 6.2. Impact of liquid flow rate on total useful heat gain for various HTLs.

- **Overall Efficiency:** The use of nanofluids dramatically boosted the overall efficiency of the DPSTC. Under optimal operating conditions (0.1 kg/s air and 0.1 kg/s liquid flow), the efficiencies reached 97% for CuO–H_2O nanofluid, 95% for MWCNT–H_2O nanofluid, and 70% for water.

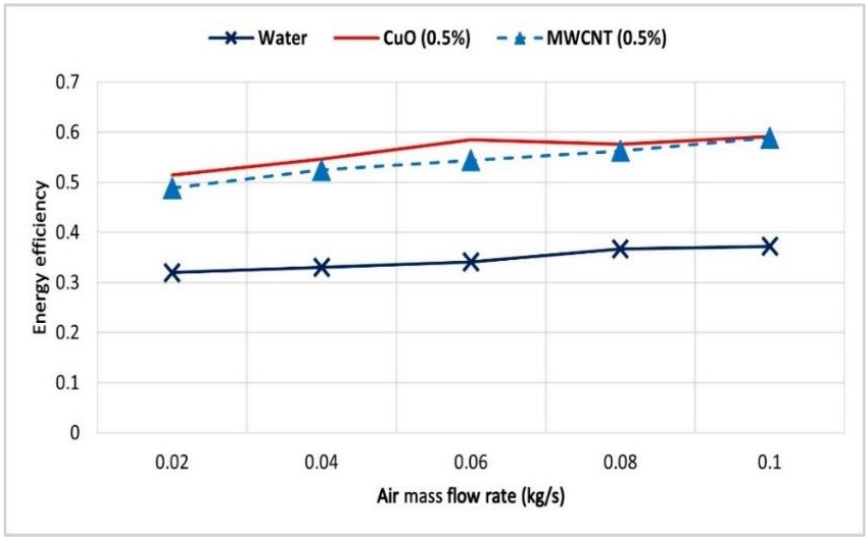

Figure 6.3. Variation of energy efficiency with airflow rate for various HTLs.

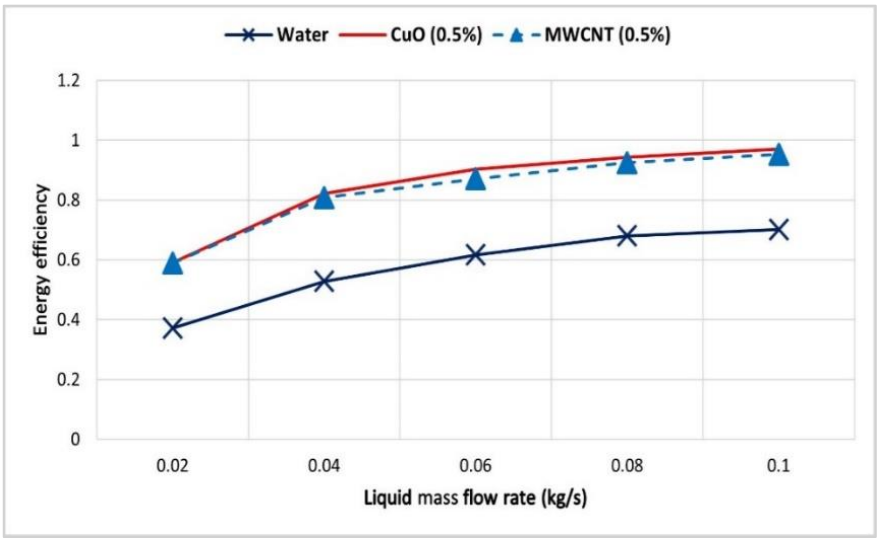

Figure 6.4. Impact of liquid flow rate on total energy efficiency for various HTLs.

Employing nanofluids, particularly CuO-H_2O at 0.5% concentration, leads to a significant advancement in the thermal performance, heat gain, and overall efficiency of a DPSTC compared to traditional water-based systems. Optimal performance is achieved at high air and liquid flow rates.

7. ENERGY, ECONOMIC, AND ECOLOGICAL ASPECTS

In this chapter, the study is divided into two parts. The first part presents a numerical investigation of the DPSTC using three hybrid nanofluids, 1%vol MWCNT-CuO/H_2O, 1%vol SWCNT-CuO/H_2O, and 0.1%vol ZrO-SiC/H_2O, building on previous work with water, Therminol, Dowtherm, and mono nanofluids. The novelty lies in applying HNFs, particularly ZrO-SiC/H_2O, which has not been previously studied in DPSTCs. The second part evaluates the obtained HNF results alongside earlier simulations, focusing on environmental performance, including fuel and CO_2 savings, as well as collector size reduction, pressure drop, and pumping power, areas not previously explored in DPSTC research [22].

7.1. Performance of Hybrid Nanofluids

The outlet liquid temperature of the DPSTC decreases with increasing mass flow rate due to reduced heat transfer time. The highest outlet temperature (50.38 °C) is achieved using SWCNT-CuO/H_2O at 0.02 kg/s, while the lowest occurs at 0.1 kg/s. The temperature drop for SWCNT-CuO/H_2O is 6.5 °C, compared to about 2.8 °C for the other tested liquids, including water.

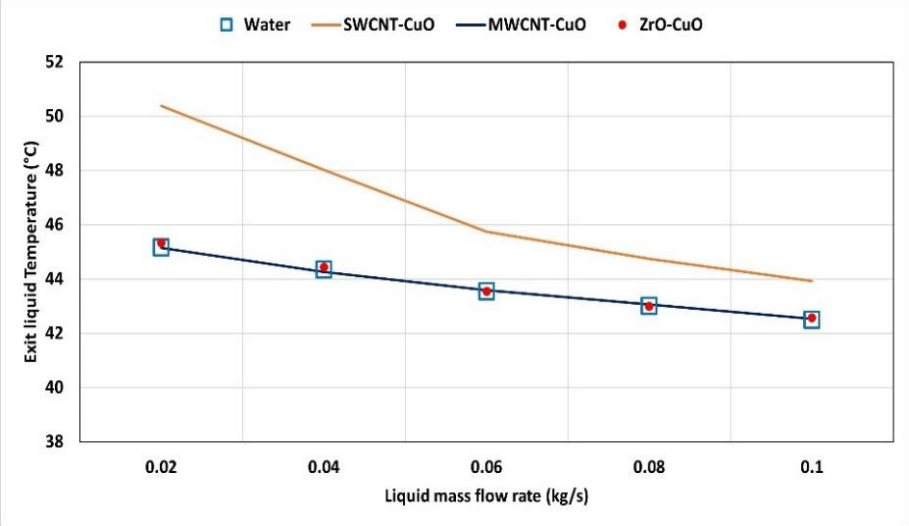

Figure 7.1. The variation of the exit liquid temperature of DPSTC with liquid flow rate.

The DPSTC total heat gain increases with higher liquid mass flow rates due to enhanced convective heat transfer. SWCNT-CuO/H_2O achieved the highest heat gain (1587.9 W), followed by ZrO-SiC/H_2O (1182 W), MWCNT-CuO/H_2O (1166.3 W), and water (1152 W), with SWCNT-CuO/H_2O showing a 37.8% improvement over water.

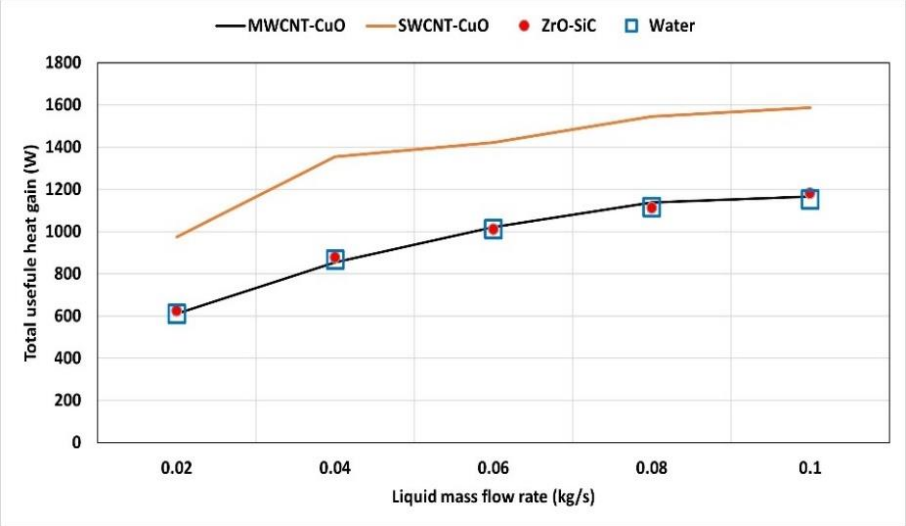

Figure 7.2. The variation of total heat gain of the DPSTC with liquid flow rate.

This indicates that SWCNT-CuO/H_2O nanofluid can be effectively applied to enhance the performance of DPSTC systems.

Previous studies [18] and [17], show that Therminol, Dowtherm, and CuO-H_2O significantly enhance DPSTC performance. At varying flow rates, Therminol and Dowtherm achieve the highest heat gains of 2962.2 W and 2812.1 W, improving performance by 157% and 144% over water, and by 86.5% and 77% compared to CuO-H_2O and SWCNT-CuO/H_2O, due to the superior thermal properties of oil-based fluids.

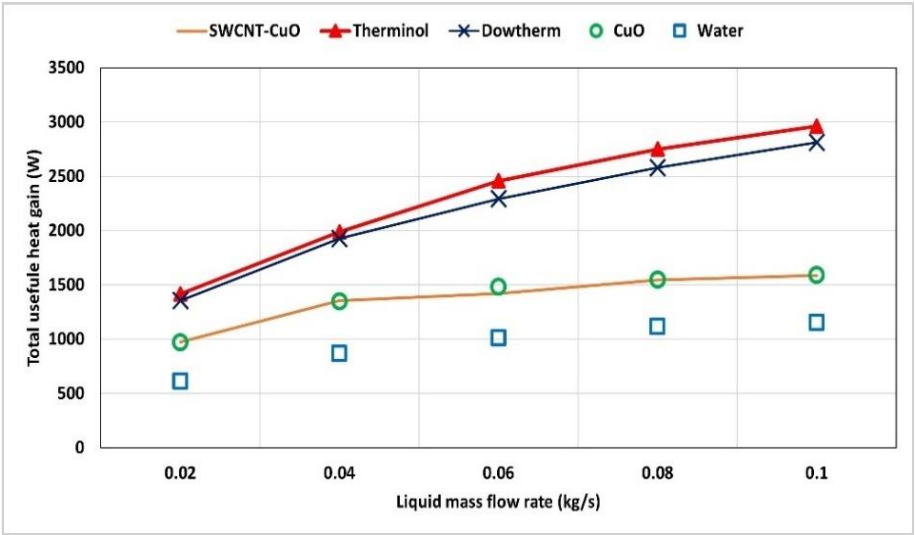

Figure 7.3. Variation of heat gain of DPSTC with various working liquids at different liquid flow rates

7.2. Comparative Environmental and Economic Analysis

The second part of this chapter presents a comprehensive environmental and economic assessment, comparing the best-performing fluids from all previous studies: Therminol and Dowtherm oils, the mono-nanofluid CuO–H_2O, the hybrid nanofluid SWCNT–CuO/H_2O, and the base fluid water.

7.2.1. DPSTC Size Reduction:

More effective fluids require less collector area to achieve the same thermal output. Therminol demonstrated the greatest potential, reducing the required area by up to 61% compared to water, followed closely by Dowtherm at 59%. The nanofluids provided more moderate reductions, with CuO–H_2O at 41.7% and SWCNT–CuO/H_2O at 37%.

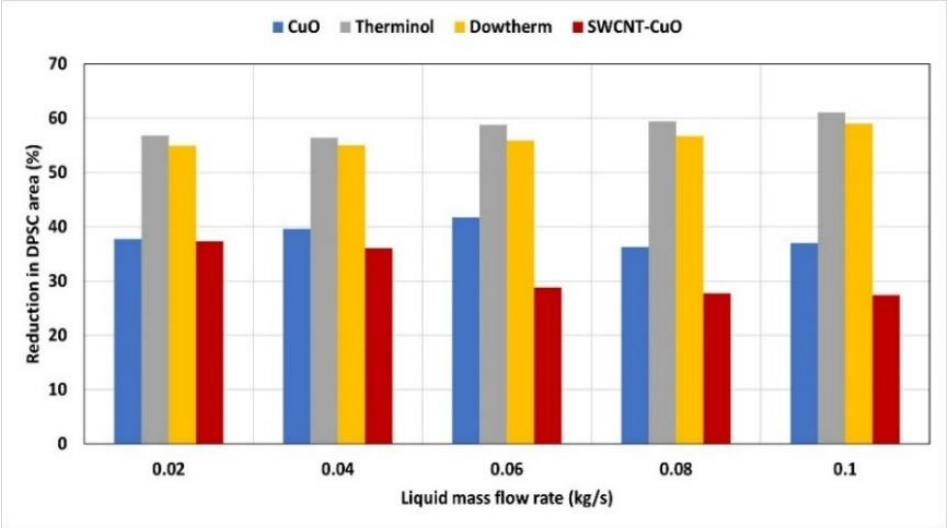

Figure 7.4. Reduction in DPSTC area for various working liquids under varying flow rates.

7.2.2. Fossil Fuel Savings and CO_2 Emission Reduction:

The heat generated by the DPSTC was evaluated in terms of potential savings if it were used to replace coal-fired, gas-fired, or electric boilers. Therminol and Dowtherm offered the greatest savings across all energy types, coal, natural gas, and electricity, while also achieving the largest reductions in CO_2 emissions. For example, under the tested conditions, Therminol could save up to 0.67 kg of coal and reduce CO_2 emissions by 1.8 kg per hour of operation compared to a coal boiler.

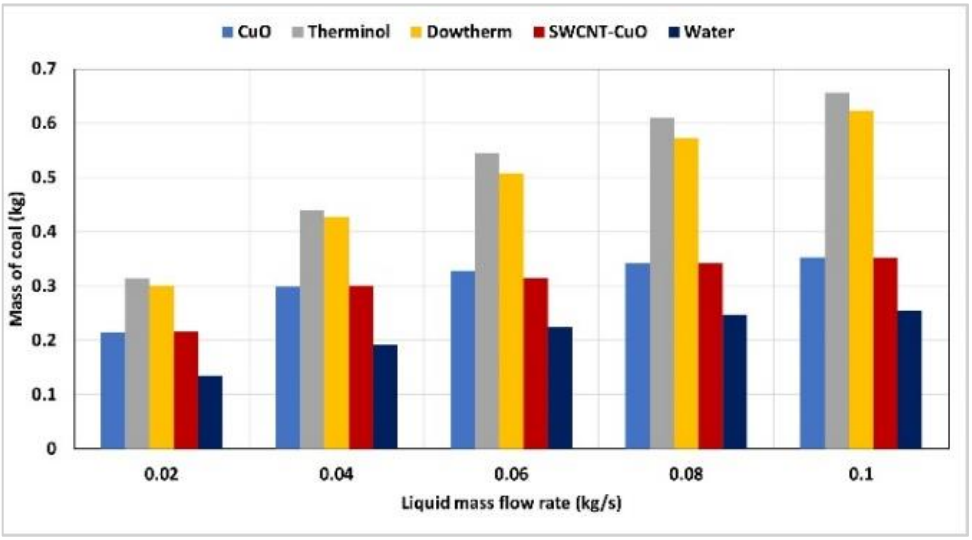

Figure 7.5. Saved coal when using DPSTC instead of a coal- fired boiler at various liquid flow rates.

Therminol and Dowtherm provide the highest DPSTC energy and CO_2 savings (up to 3.65 kWh and ~1.7 kg), followed by SWCNT-CuO and CuO nanofluids, with water yielding the least. Annual CO_2 savings are $44.5, $42.2, $23.8, and $17.3, respectively.

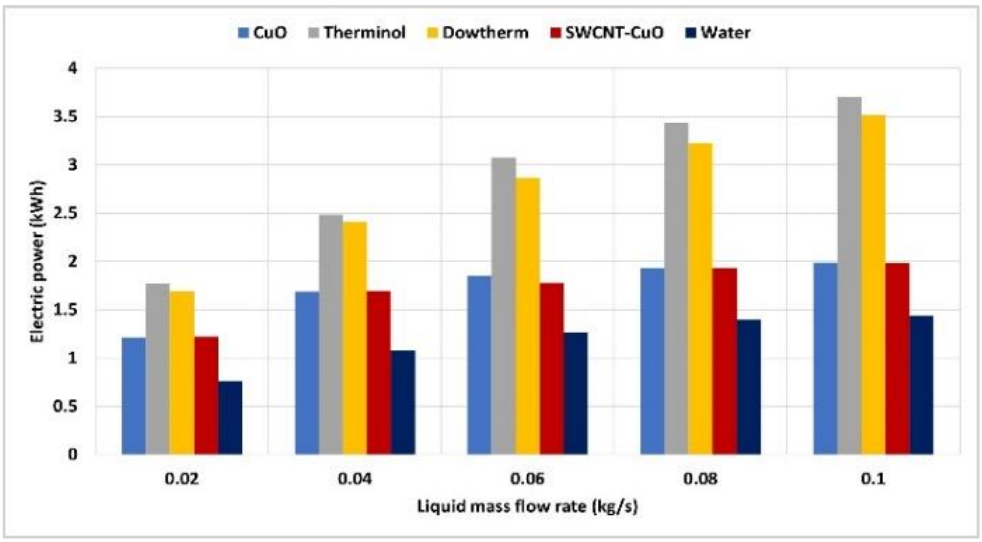

Figure 7.6. Saved power when using DPSTC instead of electric boiler at various liquid flow rates.

The gas savings and CO_2 emissions resulting from various liquids utilized in DPSTC, when compared to gas-fired boilers are shown in Figures 7.6a and b. All liquids demonstrated increased gas savings at higher flow rates, which subsequently led to greater reductions in CO_2 emissions, as these emissions are directly related to fossil fuel consumption.

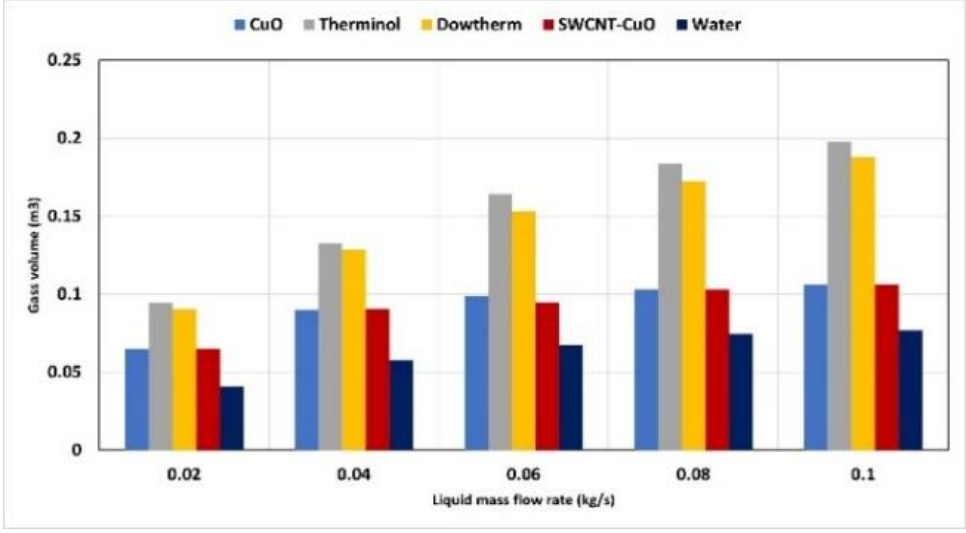

Figure 7.7. Saved gas when using DPSTC instead of electric boiler at various liquid flow rates.

7.2.3. Pressure Drop and Pumping Power

While thermal performance is critical, practical application also depends on the energy required to pump the fluid through the collector. Pumping power is directly related to the pressure drop, which is influenced by the fluid's viscosity and density.

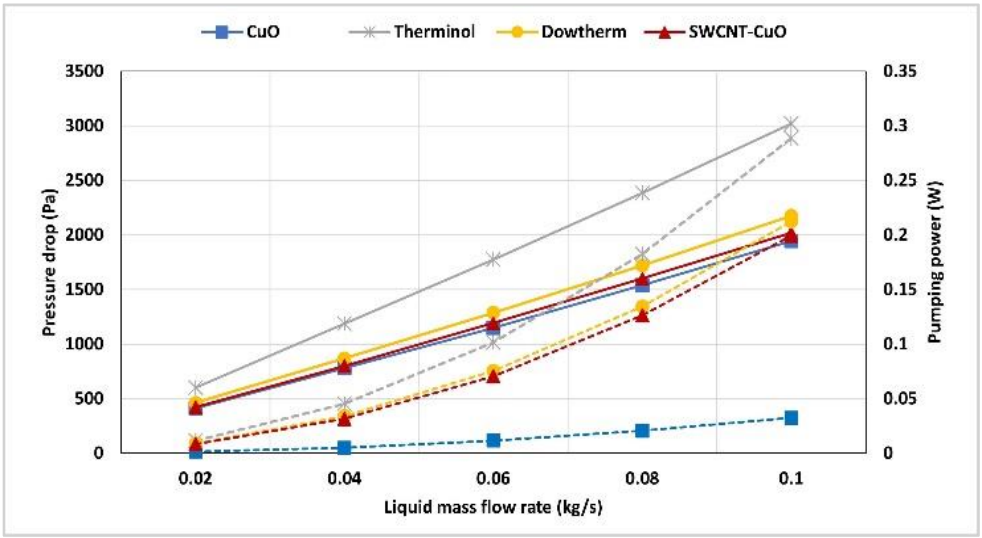

Figure 7.8. The variation of pressure drop (solid line) and pumping power (dotted line) with liquid flow rate.

In summary, Therminol required the highest pumping power (0.3 W), CuO–H_2O the lowest (0.03 W), and Dowtherm and SWCNT–CuO/H_2O were moderate (~0.2 W). Therminol and Dowtherm offer the best thermal and environmental performance but with high pumping demands, while SWCNT–CuO/H_2O is the most efficient hybrid nanofluid.

8. THESES – NEW SCIENTIFIC RESULTS

T1. I modeled the DPSTC as a parallel flow heat exchanger and developed a mathematical framework based on the ε-NTU method, applying the effectiveness equation specific to such exchangers. This novel approach, not previously used for DPSTCs, is justified by the collector's dual-channel structure. A MATLAB simulation was developed using meteorological data, and results were validated against experimental studies using RPE and ARPE metrics, confirming the model's accuracy and reduced computational complexity [P1].

T2. I developed three mathematical approaches to analyze the DPSTC. To implement these approaches, I created three MATLAB codes: C1, C2, and C3. Code C1 uses the (ε- NTU) method, C2 employs the heat removal term, and C3 uses the effectiveness term for a parallel flow heat exchanger. Each code underwent mathematical modeling, simulations, and experimental validation, showing good alignment with experimental data. I calculated the Root Mean Square Error (RMSE) and Mean Absolute Error (MAE) for each code, and found that C3 outperformed the other models with the lowest error values. As a result, C3 accurately predicts water and air outlet temperatures and the thermal performance of the DPSTC, significantly contributing to future research in this field [P2].

T3. I investigated the influence of various heat transfer fluids on the thermal behavior of DPSTC using ANSYS Fluent. I noted a considerable gap in the existing literature regarding Computational Fluid Dynamics (CFD) studies related to this type of collector, which I identified as a noteworthy innovation in my work. I evaluated three distinct working fluids: water, Therminol VP-1, and Dowtherm A. The examination of oil-based fluids, alongside conventional water, is particularly pertinent as water becomes ineffective in extreme temperatures. Additionally, the lack of research investigating these alternative fluids in DPSTC systems further underscores the originality of my study. My findings indicate that using Therminol and Dowtherm can considerably improve the overall thermal performance of the DPSTC. Therminol and Dowtherm achieve higher temperatures for the absorber plate, outlet air, and liquid [P3].

T4. I analyzed the performance of DPSTC using CFD simulations in ANSYS Fluent, employing nanofluids CuO-H_2O and MWCNT-H_2O at a 0.5% volume concentration. These nanofluids were selected based on a literature review highlighting their enhanced thermal performance in solar collectors. I compared their effectiveness to that of water, marking the novelty of this research as no prior studies have focused on these nanofluids in DPSTCs. The investigation included two phases: the first varied air flow rates while keeping other parameters constant, and the second varied liquid flow rates. I evaluated the impact of nanofluids on outlet temperatures, heat gains, and overall thermal efficiency. Additionally, I developed a MATLAB program to calculate the thermophysical properties of the nanofluids, allowing for seamless integration into the ANSYS simulation [P4].

T5. I investigated the performance of the DPSTC numerically using ANSYS Fluent, employing three different types of hybrid nanofluids: 1% vol MWCNT-CuO/H_2O, 1% vol SWCNT-CuO/H_2O, and 0.1% vol ZrO-SiC/H_2O. To date, there have been no previous studies examining the use of hybrid nanofluids (HNFs) in DPSTC, making this application a novel contribution to the field. My findings indicate that the SWCNT-CuO/H_2O fluid significantly

enhances the overall thermal performance of the DPSTC in comparison to MWCNT-CuO/H_2O and ZrO-SiC/H_2O. This suggests that the SWCNT-CuO/H_2O nanofluid can be effectively utilized in DPSTC applications [P5].

T6. I evaluated the numerical results obtained in T5 which are related to the HNFs, alongside previous simulation results presented in T4 and T3, through an environmental assessment. My analysis focused on the savings in coal, gas, and electricity, as well as the corresponding carbon dioxide emissions. Additionally, I investigated the size reduction, pressure drop, and pumping power of the DPSTC while using various liquids. These factors have not been previously addressed in the field of DPSTC, making this analysis a novel contribution to this field. I found that both Therminol and Dowtherm significantly outperform other liquids, leading to a considerable reduction in the DPSTC area. Moreover, these two fluids provide the maximum potential savings in coal, gas, and electricity compared to other liquids. However, the findings also indicate that Therminol requires the highest pumping power, followed by Dowtherm and SWCNT-CuO/H_2O, while CuO requires the least power. To minimize hydraulic losses while still achieving potential thermal benefits, it is advisable to maintain a low liquid flow rate for all liquid types [P5].

REFERENCES

[1] P. A. Owusu and S. Asumadu-Sarkodie, "A review of renewable energy sources, sustainability issues and climate change mitigation," *Cogent Eng*, vol. 3, no. 1, Dec. 2016, doi: 10.1080/23311916.2016.1167990;JOURNAL:JOURNAL:OAEN20;WGROUP:STRING:PUBLICATION.

[2] M. R. Assari, H. B. Tabrizi, H. Kavoosi, and M. Moravej, "Design and performance of dual-purpose solar collector," in *Proceedings of 3rd International Energy, Exergy and Environment Symposium*, 2006, pp. 1–5.

[3] M. AbdEl-Rady Abu-Zeid *et al.*, "Performance enhancement of flat-plate and parabolic trough solar collector using nanofluid for water heating application," *Results in Engineering*, vol. 21, p. 101673, Mar. 2024, doi: 10.1016/J.RINENG.2023.101673.

[4] D. Balamurali and M. Natarajan, "Numerical-Experimental Analysis of Solar Liquid Flat-Plate Collector with Different HTF and Internal Grooves Profiles in the Absorber Duct," *Applied Solar Energy (English translation of Geliotekhnika)*, vol. 59, no. 3, pp. 244–252, Jun. 2023, doi: 10.3103/S0003701X21101175.

[5] A. O. Borode, N. A. Ahmed, P. A. Olubambi, M. Sharifpur, and J. P. Meyer, "Investigation of the Thermal Conductivity, Viscosity, and Thermal Performance of Graphene Nanoplatelet-Alumina Hybrid Nanofluid in a Differentially Heated Cavity," *Front Energy Res*, vol. 9, p. 737915, Aug. 2021, doi: 10.3389/FENRG.2021.737915/BIBTEX.

[6] O. Al-Oran and F. Lezsovits, "Thermal performance of inserting hybrid nanofluid in parabolic trough collector," *Pollack Periodica*, vol. 16, no. 3, pp. 88–93, Apr. 2021, doi: 10.1556/606.2021.00318.

[7] M. R. Assari, H. Basirat Tabrizi, and I. Jafari, "Experimental and theoretical investigation of dual purpose solar collector," *Solar Energy*, vol. 85, no. 3, pp. 601–608, Mar. 2011, doi: 10.1016/j.solener.2011.01.006.

[8] J. A. Duffie and W. A. Beckman, *Solar engineering of thermal processes*. John Wiley & Sons, 2013.

[9] J. P. Holman, *Heat Transfer (Si Units) Sie*. Tata McGraw-Hill Education, 2008.

[10] L. H. Kumar, S. N. Kazi, H. H. Masjuki, M. N. M. Zubir, A. Jahan, and C. Bhinitha, "Energy, exergy and economic analysis of liquid flat-plate solar collector using green covalent functionalized graphene nanoplatelets," *Appl Therm Eng*, vol. 192, p. 116916, Jun. 2021, doi: 10.1016/J.APPLTHERMALENG.2021.116916.

[11] M. Amar *et al.*, "Energy, exergy and economic (3E) analysis of flat-plate solar collector using novel environmental friendly nanofluid," *Scientific Reports 2023 13:1*, vol. 13, no. 1, pp. 1–21, Jan. 2023, doi: 10.1038/s41598-023-27491-w.

[12] M. M. Hasan and K. Hriczó, "A dual-purpose solar collector as a parallel flow heat exchanger: A novel mathematical framework," *International Journal of Thermofluids*, vol. 28, p. 101322, Jul. 2025, doi: 10.1016/J.IJFT.2025.101322.

[13] O. Nematollahi, P. Alamdari, and M. R. Assari, “Experimental investigation of a dual purpose solar heating system,” *Energy Convers Manag*, vol. 78, pp. 359–366, 2014, doi: 10.1016/j.enconman.2013.10.046.

[14] M. M. Hasan and K. Hriczó, “The optimal approach of various analysis methodologies of a dual-purpose solar collector,” *Pollack Periodica*, vol. 20, no. 2, pp. 130–135, Apr. 2025, doi: 10.1556/606.2024.01244.

[15] A. A. M. Saleh and M. A. Jasim, “Experimental study of the performance of the dual purpose solar collector,” *Eng. Technol. J*, vol. 32, no. 11, pp. 2673–2683, 2014.

[16] T. O. Hodson, “Root-mean-square error (RMSE) or mean absolute error (MAE): when to use them or not,” *Geosci Model Dev*, vol. 15, no. 14, pp. 5481–5487, 2022, doi: 10.5194/gmd-15-5481-2022.

[17] M. M. Hasan and K. Hriczó, “Numerical investigation of a dual- purpose solar collector using different liquids,” *Pollack Periodica*, vol. 1, no. aop, Sep. 2025, doi: 10.1556/606.2025.01379.

[18] M. M. Hasan and K. Hriczó, “Evaluation of a dual-purpose solar collector using mono-nanofluids: A CFD simulation,” *Pollack Periodica*, vol. 1, no. aop, Oct. 2025, doi: 10.1556/606.2025.01394.

[19] H. Nabi, M. Pourfallah, M. Gholinia, and O. Jahanian, “Increasing heat transfer in flat plate solar collectors using various forms of turbulence-inducing elements and CNTs-CuO hybrid nanofluids,” *Case Studies in Thermal Engineering*, vol. 33, May 2022, doi: 10.1016/j.csite.2022.101909.

[20] E. Elshazly, A. A. Abdel-Rehim, and I. El-Mahallawi, “4E study of experimental thermal performance enhancement of flat plate solar collectors using MWCNT, Al2O3, and hybrid MWCNT/ Al2O3 nanofluids,” *Results in Engineering*, vol. 16, p. 100723, Dec. 2022, doi: 10.1016/J.RINENG.2022.100723.

[21] A. A. Hawwash, M. Ahamed, S. A. Nada, A. Radwan, and A. K. Abdel-Rahman, “Thermal Analysis of Flat Plate Solar Collector Using Different Nanofluids and Nanoparticles Percentages,” *IEEE Access*, vol. 9, pp. 52053–52066, 2021, doi: 10.1109/ACCESS.2021.3060004.

[22] M. M. Hasan and K. Hriczó, “ENERGY, ECONOMIC, AND ECOLOGICAL ASPECTS OF A DUAL-PURPOSE SOLAR COLLECTOR USING VARIOUS LIQUIDS,” *Pollack Periodica*, vol. (in press), 2026.

LIST OF PUBLICATIONS RELATED TO THE TOPIC OF THE RESEARCH FIELD

P1. M. M. Hasan and K. Hriczó, “A dual-purpose solar collector as a parallel flow heat exchanger: A novel mathematical framework,” International Journal of Thermofluids, vol. 28, p. 101322, Jul. 2025, doi: 10.1016/J.IJFT.2025.101322.

P2. M. M. Hasan and K. Hriczó, “The optimal approach of various analysis methodologies of a dual-purpose solar collector,” Pollack Periodica, vol. 20, no. 2, pp. 130–135, Apr. 2025, doi: 10.1556/606.2024.01244.

P3. M. M. Hasan and K. Hriczó, “Numerical investigation of a dual- purpose solar collector using different liquids,” Pollack Periodica, vol. 1, no. aop, Sep. 2025, doi: 10.1556/606.2025.01379.

P4. M. M. Hasan and K. Hriczó, “Evaluation of a dual-purpose solar collector using mono-nanofluids: A CFD simulation,” Pollack Periodica, vol. 1, no. aop, Oct. 2025, doi: 10.1556/606.2025.01394.

P5. M. M. Hasan and K. Hriczó, “ENERGY, ECONOMIC, AND ECOLOGICAL ASPECTS OF A DUAL-PURPOSE SOLAR COLLECTOR USING VARIOUS LIQUIDS,” Pollack Periodica, vol. (in press), 2026.

P6. M. M. Hasan and K. Hriczó, “A Literature Review of a Dual-Purpose Solar Collector,” Lecture Notes in Mechanical Engineering, pp. 302–321, 2023, doi: 10.1007/978-3-031-15211-5_26.

P7. M. M. Hasan and K. Hriczó, “Heating a greenhouse using a solar air collector assisted by thermal storage: a simulation study,” Multidiszciplináris Tudományok, vol. 12, no. 3, pp. 217–232, Nov. 2022, doi: 10.35925/J.MULTI.2022.3.20.

P8. M. M. Hasan and K. Hriczó, “Thermal performance estimation of a v-corrugated solar air heater using ann techniques,” Multidiszciplináris Tudományok, vol. 13, no. 4, pp. 42–53, Dec. 2023, doi: 10.35925/J.MULTI.2023.4.5.